Crises and Land Grabbing*

Tommaso Sonno† Davide Zufacchi‡

April 2023

Abstract

Do health crises increase land-grabbing events in developing countries? We investigate this question in the Liberian palm oil sector during the Ebola epidemic. This setting allows us to measure land-grabbing through deforestation. With a difference in discontinuity approach, we document a sharp increase in deforestation, which produced a dramatic growth in newly planted palm oil trees and a 1428% increase in palm oil exports. We also show that the probability of forest fire – the fastest way to clear forests and start new production – increased by 125% in the same period. Overall, our results indicate that crises may propel land expropriation behaviours thanks to a diversion of attention toward the emergency.

Keywords: epidemics, land grabbing, palm oil

JEL Codes: C23, F23, O13

*First version: July 2021. This version: April 2023. We are grateful for suggestions and support to Pascal Nadembega (Ministry of Health of Burkina Faso) and Luke L. Bawo, Nelson K. Dunbar, and Mohammed Kamara (Ministry of Health of Liberia). We wish to thank the UniCredit Foundation for Modigliani Research Grant funding. For their valuable comments and suggestions let us also thank Pol Antràs, Oriana Bandiera, Florin Bilbiie, Giuseppe Berlingueri, Andy Bernard, Francesco Caselli, Bruno Conte, Erika Deserrano, Joseph Emmens, Eliana La Ferrara, Jonas Hjort, Annalisa Loviglio, Massimo Morelli, Lorenzo Pandolfi, Nicola Persico, Imran Rasul, Alessandro Sforza, Vincenzo Scrutinio, Mara Squicciarini, Edoardo Teso, Francis Vella, and Gabriel Ulyssea. We are grateful for the comments of participants in seminars at the European Trade Study Group, the Online Political Economy Seminar Series, LEAP (Bocconi University), the University College London, the Jamboree 2022 (Universitat Autònoma de Barcelona), and the University of Bologna. Michael Hall provided excellent research assistance. All errors remain our own.

†University of Bologna and CEP (LSE), tommaso.sonno@unibo.it

‡University College London, davide.zufacchi.20@ucl.ac.uk

1 Introduction

Land grabbing – the acquisition or long-term lease of large areas of land by investors – is far more widespread in Africa than in any other continent (Deininger & Byerlee, 2011; De Schutter, 2011; Nolte et al., 2016). The debate is polarized between those who primarily see these as development opportunities and those concerned about the rights and livelihoods of locals (Cleveland & Cleveland, 2014). In this paper, despite not entering this specific debate, we investigate how a crisis can impact land expropriation phenomena.

Measuring land grabbing at a granular level is particularly challenging, therefore, we focus our analysis in a "special" setting, i.e. the Liberian palm oil industry during the Ebola epidemic. Due to the nature of this industry, production decisions are closely related to deforestation ones. Moreover, this sector is unique in the bureaucratic procedure towards land concession to companies, a peculiarity which will be key throughout the analysis.

The Liberian central government allocates an *area of interest* to companies. However, they need the consensus of local villages to obtain access to their land and start production. Through this consensus, a portion of an area of interest is transformed into a formal concession. In other words, even though palm oil areas of interest were allocated (allowing us to identify "treatment" areas), companies were not allowed to deforest and produce immediately on their surface. Given this setting, we try to answer the following empirical question: did companies seize the opportunity provided by the Ebola crisis to drastically increase land grabbing?

To answer this question, we compare areas just inside and just outside the palm oil areas of interest, before and after the Ebola outbreak. As mentioned above, we use deforestation to measure land grabbing. Hence, the primary source of data is MODIS Vegetation Continuous Fields. For each 1 km^2 pixel, in each period, we observe the percentage of coverage of 17, mutually exclusive, classes of land coverage, such as "Water Bodies", "Evergreen Needleleaf Forests", and "Cropland". This allows us to quantify deforestation (as a decrease in the percentage of tree coverage), as well as palm oil plantation (as increase of "Cropland", for clarification on this please refer to Appendix C). We combine this source of data with the shape of Palm Oil Areas of Interest provided by Global Forest Watch.

We observe a 5.6% increase in deforestation (approximately 1B trees lost each year), together with a rise of 125% in the likelihood of observing a fire event.[1] Simultaneously, we find a 65% increase in land devoted to crop. Three to four years after the onset of the epidemic – the time needed for a plantation to become productive – Liberia had a 1428% increase in palm oil exports with respect to the pre-Ebola period (Figure 1).

Figure 1: Liberian Palm Oil Export

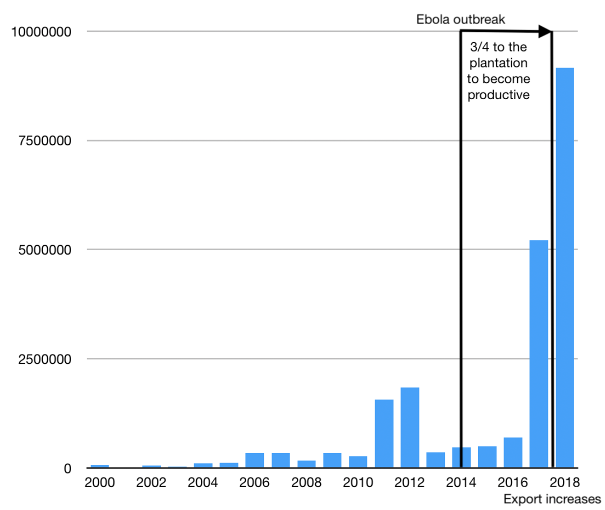

Notes: The figure presents palm oil export value from Liberia in the period from 2000 to 2018. Three-four years after the Ebola outbreak (2014), hence the time a plantation of palm oil need to become productive, there is a sharp increase in the export of this product. In particular, there is a 1428% increase in trade value with respect to the pre-Ebola period. Export data from BACI HS6 Revision 1992 (1995 - 2018).

These results suggest that companies significantly increased deforestation activities and boosted their production during the Ebola crisis. Why was this the case? In other words, how may a crisis spur land grabbing and deforestation? Extensive anecdotal evidence suggests that diversion of

[1] Agricultural enterprises tend to deforest by using controlled fires to clear areas, being it the fastest and cheapest way to switch production (Marlier et al., 2013; Emmanuel, 2000).

attention may be one of the key mechanisms behind these results (consistently with the rationale of Eisensee & Stromberg, 2007). Locals' consensus was generally agreed to in a climate of fear. Therefore, NGOs got interested and began to help local communities confront companies (usually multinationals). As a result, deforestation was highly constrained before the outbreak. This equilibrium was distorted by the virus, which redirected the NGOs efforts towards the epidemic. Consistently with this anecdotal evidence, we find: (1) evidence of a strong decrease in the NGO presence within concessions during the crisis; (2) deforestation taking place exactly in those areas interested by a reduction of NGOs presence. We also discuss alternative mechanisms, such as an increase in economic difficulty due to the crisis.

In this paper we investigate a specific setting: palm oil industry in Liberia. Although this is "special" along certain dimensions (bureaucratic procedure, direct relationship between production and deforestation), it is very similar to other contexts of extractive industries in Africa. One possible example is the mining industry in the Democratic Republic of Congo. These industries are characterized by large concessions given to companies by central governments. Moreover, they often present some degree of competition between companies and locals over natural resources. Hence, our results are at least extendable to these contexts.

This paper relates to several strands of the literature. First, the unexpected personal and environmental consequences of crises. An influential body of work has studied increased violence against women and children during pandemics (among others, Peterman et al., 2020; Bradbury-Jones & Isham, 2020), increased pregnancy rates together with a drop in school enrolment (Bandiera et al., 2019), and an increase in mistrust and economic distress (Pellecchia et al., 2015, Dhanani & Franz, 2020,Fetzer et al., 2021,Bian et al., 2022). Other studies have focused at the interaction between economic crises and crime organizations (Le Moglie & Sorrenti, 2022), health crises and Emergency Cash Assistance (Londoño-Vélez & Querubin, 2022), and long-run consequences of health crises on inequality and future labor market outcomes (Galletta & Giommoni, 2022, Ager et al., 2022). Turning to the environmental consequences, Bonardi et al. (2021) find that domestic and international lockdowns decreased PM2.5 pollution. Our paper contributes to this literature by discussing how crises may relate with land grabbing, and extracting industries more in general, in developing countries.

Second, the role of (media) attention in preventing negative behaviours. Since the seminal paper by Einsee and Stromberg (Eisensee & Stromberg, 2007), great importance has been given to attention and, in particular, media attention, in their role as "watchdogs". As an example, Durante and Zhuravskaya (2018) shows that Israeli attacks are more likely when US news were distracted by other events. Similarly, Brunetti and Weder (2003) find evidence that media attention is associated with lower corruption. This is strictly connected with the finance literature investigating whether private companies release negative earnings reports in periods of low market attention (Patell & Wolfson, 1982, DellaVigna & Pollet, 2009, DeHaan, Shevlin, & Thornock, 2015, Michaely, Rubin, & Vedrashko, 2016, Blankespoor, deHaan, & Marinovic, 2020). We contribute to this literature both connecting the idea of attention diversion to land grabbing phenomena and discussing about NGOs attention rather than media one.

Third, although in this work we do not analyse the effects of land grabbing on the locals, the literature suggests that the consequences of deforestation are multiple and pervasive, both socio-economically and environmentally, and they are often associated with large-scale land acquisitions (Davis et al., 2015, Probst et al., 2020, Nepstad et al., 1999). If one adds even the severe health repercussions of controlled forest fires (Marlier et al., 2013, Johnston et al., 2021, Rangel & Vogl, 2019, Currie et al., 2009), the long-lasting consequences of the rapacity of these companies become a prime issue.

The paper is structured as follows. Section 2 presents the background and section 3 the data. Results are then described in section 4. Section 5 concludes.

2 Background

With the end to the country's second civil war (1999-2003), Liberia turned to its natural resource endowments to galvanize the economy. In 2012, the IMF estimated returns from palm oil and iron ore concessions in Liberia as high as US$ 2 billions dollars in the period up to 2020, with additional payments to follow.[2]

Palm oil sector in Liberia is particularly suitable to investigate the impact of a health crisis on land grabbing and deforestation for two main reasons. First, the connection between land grabbing and deforestation. Without granular data on land grabbing, it is difficult to track this phenomenon. This becomes particularly hard when studying exploitative behaviours, which, by their nature, are meant to be concealed. For this reason, an indirect measure of these activities is needed, despite it being rarely available. In the palm oil sector, instead, we can retrieve land grabbing decisions from deforestation, which is observable at the very granular level. Deforestation is, indeed, a main step in the palm oil production process. Second, the bureaucratic procedure towards land concession is peculiar, as we explain in detail below.

The first step to large-scale production of palm oil in Liberia is to contract a land with the central government. As an example, two major palm oil agreements in 2009 and 2010 granted a total of 440,000 ha to foreign multinational company. These large piece of land are called "areas of interest". However, this government agreement does not give companies any production right. Before converting land into plantations, the companies must win the consensus of the local communities. Specifically, each company has to sign a Memoranda of Understanding with them. The area is then transformed into a concession, where the multinational can deforest and start production. Areas of interest are those interested by palm oil activities, hence, our "treatment" zones. Since companies have no immediate production right on them, if we observe a sharp increase in deforestation within these areas during the crisis, this is evidence of large increase of

[2] Source: Smell-NoTaste.

Memoranda of Understandings.[3]

From 2010 to 2014 one of the two leading palm oil multinational company signed agreements for a total area of approximately 298 km^2. In the three months between August and October 2014, just after the epidemic outbreak, it increased the number of agreements by 45% (Global Witness, 2015). To visualize the phenomenon, Figure 2 displays deforestation events for a palm oil area of interest in Liberia. In the first map, top-left, pixels (30$\times$30 meters) are colored red if a deforestation event happened between 2001 and 2010, and one year is added to each successive map.[4] As one can see, subsequent deforestation events were quite rare within in the area of interest, up to 2013. In 2014 and 2015, there was a quantum leap in deforestation. Starting from this evidence, in this paper we investigate whether the Ebola outbreak may have spurred rapacity behaviours of palm oil companies in Liberia.

Figure 2: Ebola and deforestation

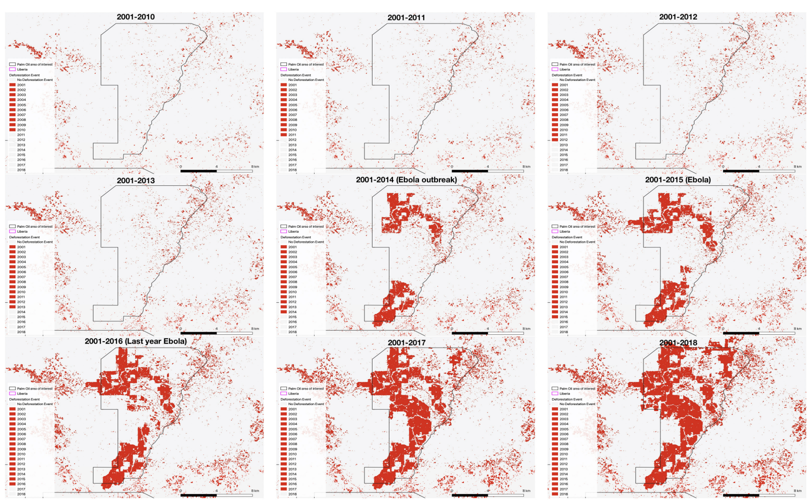

Notes: The figure presents the deforestation process within one palm oil area of interest in Liberia. In particular, in the first map, top-left, pixels (30$\times$30 meters) are coloured red if a deforestation event occurred between 2001 and 2010. In the rest, one year is added for each successive map. As one can see, deforestation events were quite rare within the area of interest up to 2013, but in 2014 and 2015 there was a quantum leap.

[3] An alternative story could have been an increase in palm oil price, something we do not observe in the data (Figure A1 in Appendix A).

[4] In order to easily visualize tree cover loss, for this picture we use data that contain areas of tree cover loss at approximately 30$\times$ 30-meter resolution (Hansen et al., 2013).

3 Data

We explore the interaction between the Ebola epidemic, deforestation, and concessionary firms in Liberia. This requires geolocalized data on the percentage of trees and palm oil areas of interests, plus the additional data described below. The resulting dataset is structured as a full grid of Liberia. Each grid has an area of approximately 1 km^2, for a total of 98,123 cells observed for nine years.

Land Cover Data. The primary source of data is MODIS Vegetation Continuous Fields (Dimiceli et al., 2015), which offers a quantitative portrayal of the yearly percentage of land cover at 0.05-degree pixel resolution for the entire globe for the period 2000-2020. In particular, for each pixel, we observe the percentage covered by each class as recorded by the International Geosphere-Biosphere Programme (IGBP). This divides the types of land cover into 17, mutually exclusive, classes precisely defined, such as "Water Bodies" (permanent water bodies) or "Evergreen Needleleaf Forests" (evergreen conifer trees with canopy >2m). Figure A2 in Appendix A shows a cross-section plot of the most wide spread class in Liberia in 2010: "Evergreen Broadleaf Forests". This is our main dependent variable and, since Evergreen Broadleaf Forest is the most common type of tree cover in Liberia, we here use the term percentage of tree cover to indicate the percentage of Evergreen Broeadleaf Forest without loss of generality. The main advantage of this source of data is that we can observe the increase in deforestation, measured as decrease in the percentage of tree cover. Moreover, this data allows one to measure the increase in palm oil cultivation, measured as the percentage cover of "Croplands".[5]

Palm Oil Areas of Interest. To define whether a cell belongs to an area of interest, we use data from Global Forest Watch, which give information about the shape, location, and ownership of palm oil areas in Liberia.[6] No information about years of concession is provided. Therefore,

[5] Tan, Kanniah, and Cracknell (2014) provide a way of linking plants' age and canopy size. According to their study, palm oil trees have little canopy when they are young (<1m radius in the first 2-3 years of life), therefore, *newly* planted palm oil trees can be classified as "Croplands".

[6] Global Forest Watch. 2019. World Resources Institute. Accessed on 23/07/2020.

we use the ownership data to retrieve this information. On the basis of several technical reports, we can conclude that all the areas of interest in our sample were granted by 2010 at the latest.[7] To avoid potential endogeneity arising from the opening of new areas, we restrict our sample to the period between 2010 and 2018. More information about the palm oil companies can be found in Appendix C.

Fire data. Granular data about fire events is obtained from USGS - MCD64A1 (Version 6). This is a monthly, global, gridded 500m product containing per-pixel burned-area. For each of these pixels, and each month, we observe whether there was a fire event or not.

NGO data. Obtaining geo-localized measures of NGOs presence is particularly hard. We do it indirectly by using the Demographic and Health Survey (DHS), phase VI (2011), VII (2013), and VIII (2016). In particular, we define an NGO being present in a certain cell-year if there is at least one DHS respondent declaring that an NGO has sprayed his dwelling in the previous year.

Other data. For information about the sources of other data (e.g. population, weather) used in this paper please refer to Appendix D.

Descriptive statistics can be found in Appendix E.

4 Empirical Analysis

In this section, we study the differential impact of Ebola on tree coverage within and outside areas of interest. Using two alternative methodologies, we show that (i) these areas undergo a sharper decline in tree coverage during the epidemic than before it, and (ii) fire events are more frequent during epidemic years. These pieces of evidence suggest a scenario in which the health crisis represented a chance for increasing land grabbing.

[7] For example, Making concessions in Liberia - Agriculture (Tamasin Ford), accessible here.

4.1 Preliminary evidence

The setting described in section 2 clearly suggests the difference-in-difference approach, so, we use a linear regression to estimate changes in cells' tree coverage in areas of interest during the Ebola epidemic, compared with both non-epidemic years and with non-interest areas. Denoting a generic cell k, with $k \in r$, where r is a region and t a generic year, and ignoring controls, our regression model is:

$$T_{krt} = \alpha + \beta\ E_t \times A_{kr} + \mu_k + \mu_{rt} + u_{krt} \tag{1}$$

where T_{krt} denotes the percentage of evergreen broadleaf forest in cell k in region r in year t, E_t is a dummy equal to one in 2014 and 2015, A_{kr} is a dummy equal to one for cells in an area of interest. Columns 1 and 2 of Table 1 summarizes results of model (1). All regressions include the Standardized Precipitation Evapotranspiration Index (SPEI) at cell level, cell (μ_k) and region$\times$year (μ_{rt}) fixed effects. This section replicates this exact table for our two identification methods: difference in difference and difference in discontinuity. It is also replicated in a sharp geographic regression discontinuity approach (presented in Appendix F). Column 1 shows that during the Ebola epidemic, within the areas of interest the percentage of tree cover decreases (by almost 0.3% with respect to the sample mean). Column 2 focuses on the potential use of controlled fires to clear areas targeted for new productions. To do so, we replicate column 1 replacing the dependent variable with a dummy assuming value one when in a cell there is at least one fire event during the year. During the epidemic, in the areas of interest, we observe a significantly higher likelihood of a fire event (+74%).

The difference-in-difference identification strategy depends on the parallel trend assumption. This requires that the same trend of no treatment before/after Ebola and within/outside areas of interest. Equivalently, cells within areas of interest should have had the same trend in tree cover and fire events as those outside the palm oil areas. This assumption, in this context, is particularly strong. Palm oil areas of interest have a maximum radius of 10 km, meaning that cells at the heart of them might differ from those at the boundaries. For this reason, the trends of these cells might have been different over time, even without health crisis. To address this identification issue, one should compare cells that are close to another. In other words, we need a more localized identification strategy.

Table 1: Difference in Difference and Difference in Discontinuities

	Diff in Diff		Diff in Disc	
	(1)	(2)	(3)	(4)
Dep. Variable	% Trees	Fire event	% Trees	Fire event
Ebola × Area of Interest	-0.116**	0.0172***	-1.952***	0.0277**
	(0.0489)	(0.00206)	(0.635)	(0.0134)
Observations	880821	880357	44577	155124
R-squared	0.979	0.228	0.980	0.209
Cell FE	Yes	Yes	Yes	Yes
Region × Year FE	Yes	Yes	Yes	Yes
SPEI	Yes	Yes	Yes	Yes
Mean dependent	48.15	0.0232	35.10	0.0223

Notes: MWFE estimator. HDFE local linear regression. Sample restricted to be within the optimal bandwidth computed following the procedure outlined by Calonico et al., 2019. Observations weighted by an exponential kernel function of distance and bandwidth. Standard errors in parentheses. ***,**,* = indicate significance at the 1, 5, and 10% level, respectively. Standard errors clustered at the cell level in all models. *Ebola* is a dummy equal to one in 2014 and 2015. *Area of Interest* is a dummy equal to one for cells in an area of interest.

4.2 Difference in Discontinuities

The difference-in-discontinuity approach compares cells just outside and just inside the palm oil areas of interest. Given their proximity, they are very likely to be similar. Thus by comparing these two groups one could retrieve the effects on our dependent variables. The most common identification method based on this reasoning is regression discontinuity, which we present in Appendix F. However, this completely neglects the time dimension, which is fundamental for the setting presented in Section 2. Moreover, the non-random nature of the boundaries of the palm oil areas of interest casts doubt on the continuity of potential outcomes at the boundary, thus invalidating the sharp geographic regression discontinuity results. The solution to this identification problem comes from the combination of the two methods mentioned above (difference in difference and regression discontinuity) into a different one: difference in discontinuities. The general concept of this strategy is to perform a local difference in difference. It compares trends of cells just outside and just inside the palm oil areas of interest. This overcomes the limitation of the first method, since it is a local estimation, meaning that we consider only cells at the boundaries, and it also solves the shortcomings of the second method by comparing trends and not levels. This allows us to include cells within concessions in the control group (and thus to deal with the non-randomness of the concession boundaries) and to compare periods before and after the Ebola outbreak.

This identification strategy relies on a relaxed version of the two assumptions typical of the constituent methods, namely parallel trends and continuity. First, it requires continuity of potential outcomes to the right and to the left of the boundaries, but not necessarily *at* the boundary. In other words, it is robust to the potential discontinuity of the potential outcomes' conditional means, which would invalidate the sharp geographic regression discontinuity approach. Second, it requires a local version of the parallel trend assumption. Locally, we require the same trend of no treatment before and after Ebola, just within and just outside concessions in the absence of the health crisis. By comparing adjacent cells, this local parallel trend is more likely to be subsist than is the global one. Appendix G describes in detail the assumptions and provides an intuitive proof of identification.

Due to the local nature of the identification strategy, we restrict the sample to cells within 10 km of the boundary of the areas of interest (Figure A4 in Appendix F shows the geographic dimension of this restricted sample).[8] Moreover, when performing the analysis on fire events, we exclude from the sample a buffer zone of radius equal to the diagonal of a cell (1.42 km) within and outside the areas of interest for three main reasons: (i) the possibility of non enforcement of

[8]The distance from cells to boundaries is computed in the following way: it is the (shortest) path from centroids of each cell to areas boundaries. 10 km is the maximum distance between a cell within an area of interest and its boundary. Hence, by restricting the sample to cells within 10 km of the borders we are sure to include in the sample all cells within the "treatment" group.

boundaries (i.e., they are not "visible" on the ground), and (ii) even though these are "controlled" fires, it is complicated to make them respect a (non visible) boundary exactly, to the meter.[9] Table A1 in Appendix B presents some descriptive statistics of the dependent variables in the restricted sample, as well as the difference between inside and outside the areas of interest.

To estimate the local linear difference-in-discontinuities treatment effect, we combine the procedure outlined by Calonico et al. (2019) with a time dimension. In other words, we run local linear regressions of our outcome variable Y in cell k belonging to region r in year t (Y_{krt}) on a constant, a dummy indicating areas of interest A_{kr}, the distance D_k as well as their interaction, and we combine this model with the dummy variable E_t indicating Ebola years (2014 and 2015) to introduce the time dimension. As is standard, we use only units within bias-robust and optimally chosen bandwidths, and we weight observations by a kernel function according to their distance from the cutoff.[10] Hence, we estimate the following model:

$$Y_{krt} = \alpha_0 + \tau_0 A_{kr} + \beta_0 D_k + \gamma_0 A_{kr} \times D_k + E_t(\alpha_1 + \tau_1 A_{kr} + \beta_1 D_k + \gamma_1 A_{kr} \times D_k) + u_{krt}. \quad (2)$$

The coefficient of interest of the difference in discontinuity is τ_1. The results are summarized in columns 3 and 4 of Table 1, robustness tests reported in Appendix B, tables A3 and A2. Column 3 shows that, near the boundaries, within areas of interest, during Ebola, there was a decrease in tree cover. This decrease is considerable in magnitude, approximately 5.6% of the sample mean.[11]

[9] In setting the dimension of the buffer, we face a classical bias-noise trade-off. If one increase the size of the buffer, there will be less noise but less similar cells, hence a greater bias. On the other hand, if one decreases it, there will be more noise, for the reasons above, but less bias in the estimates. In the main specification we favor the bias dimension. A sensitivity analysis is presented in Appendix B, Table A3.

[10] Specifically, the optimally chosen bandwidths h are such that $D_k \in [-h, h']$. Moreover, the exponential kernel function is of the form: $K(D/h) = \frac{e^{h-|D|}}{e}$. Sensitivity to other kernel functions, as well as other buffer radii are presented in Appendix B, Tables A2 and A3 respectively. Since the bandwidth is chosen optimally for the two dependent variables (% Trees and Fire event), the number of observations in Table 1 differs between columns 1-2 and 3-4.

[11] This coefficient may seem small on a first sight, however, its magnitude is very large in terms of real trees lost. To see why this is the case, let's back up the average number of threes cut as a result of these rapacity behaviours. In Liberia there is an average tree density of 285,600 trees per km^2 (source: National Forest Inventory 2018/2019). Therefore, on average, for each cell, approximately 2,600 trees were cut down (285,600×5.6%). Multiplying this

Column 4 explores the other mechanism in play: controlled fires. During Ebola, within areas of interest, with respect to cells just outside, there is an increase in the probability of a fire event of more than 125%.

4.3 Sensitivity

Table A3 in Appendix B replicates the difference-in-discontinuity analysis for different choices of internal buffer. Results with this dependent variable are quantitatively and qualitatively similar across different radii. Table A2 presents the sensitivity of the results to the inclusion of controls and other fixed effects, to change in the kernel weighting function, and to computation of the standard errors. The results are robust to the inclusion of different weather controls (rainfall, temperature, humidity, vapor pressure, PM25), cell characteristics (nightlight and population) and other fixed effects (no cell, no region × year, province). Different choices for the kernel function (no weighting, triangular, uniform and epanechnikov) produced similar results. The results are also unchanged when standard errors are clustered at the province level, when robust standard errors are used, and when their spatial and time correlation is considered as in Colella et al. (2019), who elaborated on Conley (1999). Finally, the results are also robust to the use of a different, more disaggregated, source of data for the percentage of tree cover.[12]

To assess the weaker parallel trend assumption described, we use a staggered difference-in-discontinuity approach, with 2013 as reference year. In particular, we modify model 2 as follows:

$$Y_{krt} = \alpha_0 + \tau_0 A_{kr} + \beta_0 D_k + \gamma_0 A_{kr} \times D_k + \sum_{t=2010}^{2018} T_t(\alpha_1 + \tau_1 A_{kr} + \beta_1 D_k + \gamma_1 A_{kr} \times D_k) + u_{krt}. \quad (3)$$

number by the total number of cells within areas of interest (approximately 88,000), we obtain the impressive number of 1407 million trees lost.

[12] In this robustness we use another MODIS' product. This is more dis-aggregated (30m × 30m pixel, we aggregate this at the 1km^2 cells) but it displays only the percentage of tree cover for each pixel and not of the 17 IGBP differentiation we use in our analysis. A cross-section plot of this more granular dependent variable is depicted in Figure A5 in Appendix A.

The results are summarized in Figure 3, which presents $\tau_{1,t}\ \forall t = 2011, 2016$.[13] There is no pre-trend neither in deforestation or fire events within the areas of interest. In other words, close to the boundaries, there is no significant difference in tree cover or fire events for the years before the Ebola outbreak. But, starting in 2014, there in considerably less tree cover and fire events are significantly more likely in cells inside the areas of interest than outside.

Figure 3: Staggered coefficients

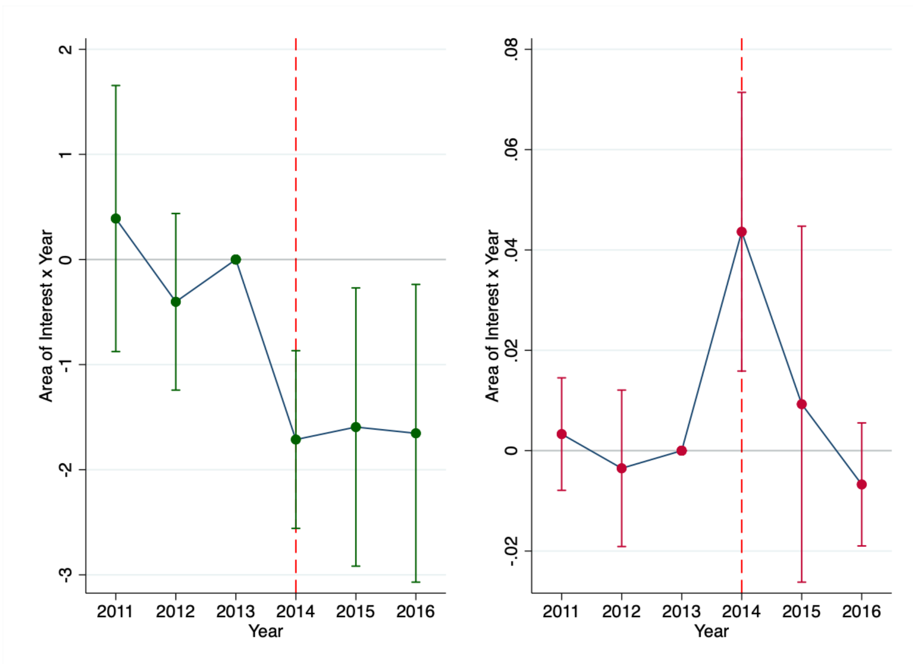

Notes: The figure presents coefficients from the staggered difference-in-discontinuity, with 2013 as reference year. On the left, the dependent variable is the percentage of tree coverage. Instead, on the right, the dummy variable indicating the presence of a fire event. MWFE estimator. HDFE Linear regression. Sample (10-km + 1.42km internal buffer) restricted to be within the optimal bandwidth computed following the procedure outlined by Calonico et al., 2019. Cell and region $\times$ year FE are added in all regressions. Standard errors clustered at the cell level. 95% confidence intervals shown.

Considering the extensive literature on ethnic groups in developing countries , one could wonder whether they play a role in our analysis. In Appendix H we replicate our analysis, both with a difference in difference and a difference in discontinuity approach and we show that, during Ebola and within areas of interest, the decrease in tree coverage and the increase in fire events

[13] The regression includes all years, but for graphical purposes here we present the coefficients only for 2011-2016.

are strongly amplified in areas where we observe ethnic groups not represented in the government.

4.4 Discussion and Mechanism

In section 2 we stressed that, in the palm oil sector, deforestation was a good indirect measure land grabbing and companies activities. This relies on the very strong connection between deforestation and production in this sector. This is a fairly logical argument. Nevertheless, given the importance it plays in our analysis, we try to provide some evidence of it in the following. In particular, we investigate whether this deforestation translated to increase production. To enquire into this, we use a particular feature of our dependent variable. Out data give, for each pixel, the cover percentage of 17 typologies of land-cover classes (see Section 3). Hence, we can monitor whether - together with a decrease in evergreen broadleaf forests - we also find an increase in the type of cultivation associated mostly with *newly planted* palm oil trees, namely, “cropland”.[14] The results, summarized in Table 2, confirm that the extensively documented *decrease* in tree cover is paired with a 65% *increase* in newly planted palm oil trees (i.e. Cropland), which is in line with the impressive +1428% jump in Liberian palm oil exports in the next 2-3 years.

Table 2: Cropland

	(1)	(2)
Dep. Variable: % Cropland	Difference in Difference	Difference in Discontinuities
Ebola × Area of Interest	0.271***	0.310***
	(0.0133)	(0.0442)
Observations	880821	117432
R-squared	0.807	0.650
Cell FE	Yes	Yes
Region × Year FE	Yes	Yes
SPEI	Yes	Yes
Mean dependent	0.154	0.474

Notes: MWFE estimator. HDFE local linear regression. Difference in Difference analysis in column (1); difference in discontinuities in column (2). Sample restricted to be within the optimal bandwidth computed following the procedure outlined by Calonico et al., 2019 in columns (2). Observations weighted through an exponential kernel function of distance and bandwidth in column (2). Standard errors in parentheses. ***,**,* = indicate significance at the 1, 5, and 10% level, respectively. Standard errors clustered at the cell level in all models. *Ebola* is a dummy equal to one in 2014 and 2015. *Area of Interest* is a dummy equal to one for cells in an area of interest.

[14] Palm Oil trees are not the only type of cultivation included in this class. For a more detailed discussion about this point please refer to Appendix C.

Results presented so far suggest that palm oil multinationals engaged land grabs and increased their production. But how may a crisis spur these activities? What is the mechanism behind these results? Substantial anecdotal evidence suggests that this may be due to a diversion of attention of local and international NGOs (Global Witness, 2015; RSPO complain; Forest Peoples Programme, 2015). As is often the case in these situations, the Memoranda of Understandings were signed in a climate of fear. Many members of the village communities were arrested because they refused consent. This evidence suggests that several NGOs got interested in the problem. They visited the communities, monitored corporations' operations and assisted locals in filing complaints to the authorities. As a result of their activities, exploitative behaviours by palm oil companies were significantly constrained.[15] However, Ebola redirected NGOs efforts towards the epidemic. Hence, villages were left without reliable information on the corporations' intentions or protection. In other words, anecdotal evidence suggests that this diversion of NGOs' attention, caused by the Ebola outbreak, spurred land grabbing and deforestation.

To test this hypothesis, one needs a geo-localized information of NGOs presence and activity before and after the Ebola outbreak. As expected, this is particularly hard to obtain. Though imperfectly, we try to indirectly measure NGOs presence through the Demographic and Health Survey (DHS), phase VI (2011), VII (2013), and VIII (2016), as explained in section 3. In particular, we say that an NGO is present in a certain cell-year if there, in the following period, is at least one DHS respondent declaring that an NGO sprayed his dwelling against mosquitoes in the previous 12 months. This measure has several limitations. First, it is not specific to NGOs working in the palm oil sector. Second, it is highly noisy, depending on a sub-question of an unrelated survey. Third, its geographic coverage is limited to the presence of DHS "areas". However,

[15] See, for example, Global Witness (2015); RSPO complain; Hollow promises. From the Global Witness (2015): "Prior to Ebola local NGOs provided support [...]. During the Ebola outbreak, however, this oversight and support to communities decreased significantly [...] deprived of NGO support, it is clear that the conditions for genuine FPIC (free prior informed consent) to be obtained did not exist during the Ebola crisis." Also, interviews with people living in the areas describing how the local authorities (often village chefs) took advantage of people's illiteracy to convince them to sign the Memorandum of Understanding (minute 6:52 or 7:55): interviews.

although its limitation, it can still be useful to corroborate the hypothesis about the mechanism behind our results. Figure A6 in Appendix A shows the geographical distribution of DHS areas over the different waves. As one can see, there is substantial geographical variation, and there are several respondents within palm oil areas of interest. We perform a two step analysis. First, we study NGOs presence before and after Ebola outbreak, within and outside palm oil areas of interest. Second, we augment our model 2 with the NGOs measure to see how this interacts with deforestation.

Before Ebola, the average NGOs presence was higher within areas of interest than outside them, consistently with these helping the communities. However, this is not true anymore during the health crisis (Table A4, Appendix A). As a result, we observe a 180% decrease in the probability of observing an NGO within areas of interest during Ebola (Table A5, column 2, Appendix A). This result is robust to the inclusion of different control variables (population, nightlights, and rain), fixed effects (column 3), and restriction of the sample to the one in the difference-in-discontinuities analysis (columns 4-5).[16] In columns 6-7 we take in consideration the dislocation of DHS areas. Indeed, to preserve privacy of respondents, the DHS team dislocates the areas up to 5km in rural areas. Hence, here we delete from the samples cells within 5km from areas of interest boundaries. Results are unchanged. Overall, results presented are consistent with a lower presence of NGOs during Ebola in areas of interests.

To see how this interacts with deforestation, we interact model 2 with the NGOs measure. Specifically, we construct a dummy equal to 1 if there is a decrease in NGOs presence within the area of interest considered. By doing so, we compare deforestation (within areas of interest, during Ebola) in areas with an actual decrease in NGOs with those in which this is not true. The only difference between the empirical specification used here and the one used in section 4.2 is that here we eliminate the 5km area outside areas of interests to deal with DHS dislocation.

[16] If we restrict the sample to cell-years with at least one DHS respondent we lack sufficient power to perform standard analysis. Nevertheless, taking a simple difference in means, we still observe a decrease in NGOs presence.

Results are summarized in Figure 4. As in the previous section, within areas of interest, during Ebola, we observe a lower percentage of tree cover. However, this changes when we include the interaction with the change in NGO measure. In particular, all the effect is "captured" by this interaction, consistently with these areas of interest being the ones targeted by deforestation due to NGOs' diversion. This result is robust to different kernel weighting functions, as well as to the inclusion of additional controls that can explain NGOs presence, such as rain and nightlights.[17]

Results presented are consistent with the diversion of NGOs attention as mechanism behind the relationship between land grabbing and crises. This mechanism sheds light on how crises can spur deforestation in fragile countries by *diverting* the national/international *limited attention* (Gabaix & Laibson, 2006; Chetty, Looney, & Kroft, 2009; DellaVigna, 2009) towards the crisis. Moreover, this sheds light also on how effective correct information is in preventing corporations' rent-seeking in fragile countries. Most fragile countries have regulations limiting MNEs' activities, but asymmetric information results in weak enforcement. Providing correct information about the consequences of agreements with these companies may strengthen enforcement, moderating the adverse impact of their presence while retaining the potential benefits for economic development. Providing sound information, in other words, could be an extraordinarily cost-effective solution. Of course, alternative mechanisms may play a role too. One example could be starvation. Ebola severely affected village families' income, making the weaker ones keener to accept the agreements, even though the benefits were limited. Another example may be a change in household preferences after the health crisis.

5 Conclusions

In this paper we study the palm oil sector in Liberia to understand whether crises may increase land grabbing. This setting is "special" because it allows us to measure land grabbing through

[17] One may be worried that this results are driven by NGOs being more present in areas with ethnic minorities, however, the correlation between our NGO measure and the presence of an ethnic minority is very low (-0.0024).

Figure 4: Deforestation and NGO

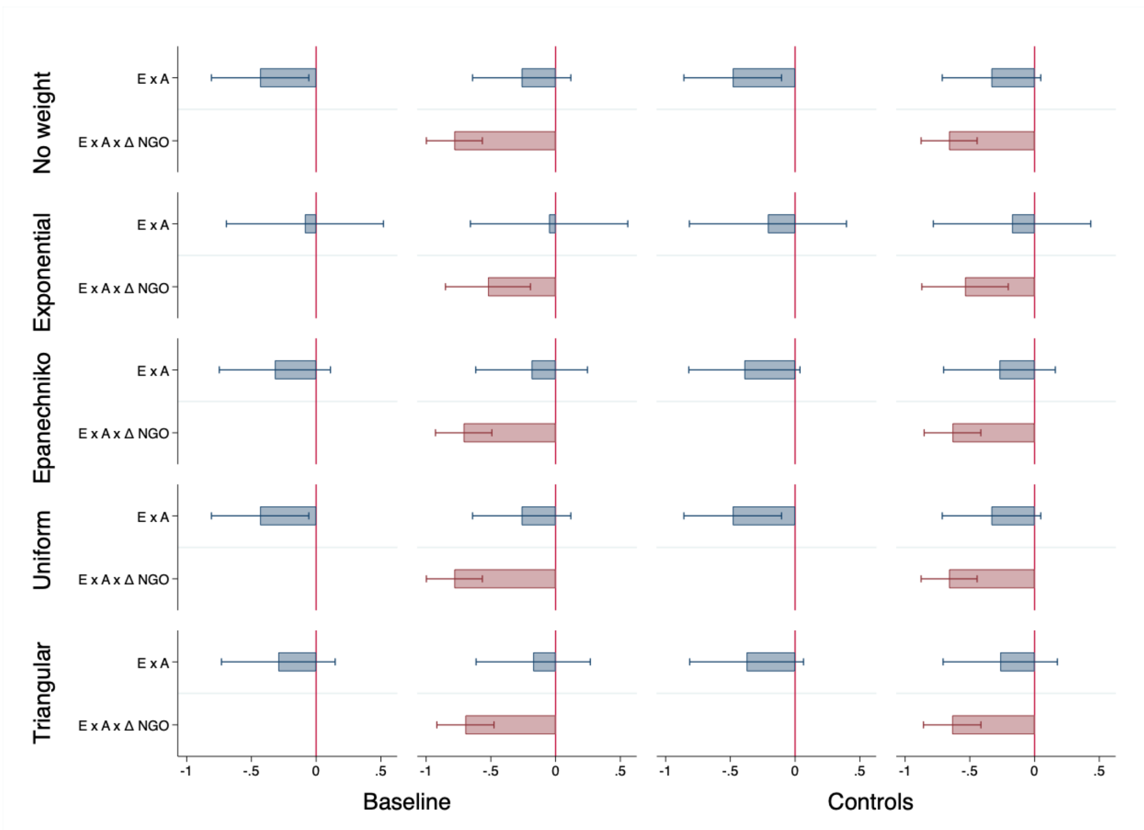

Notes: The figure coefficients from diff-in-disc regressions on deforestation and NGOs presence. MWFE estimator. HDFE Linear regression. Dependent variable is the percentage of tree coverage. E is the dummy for the Ebola (2014 and 2015). A stands for *Area of Interest*, a dummy equal to one for cells in an area of interest. Δ NGO is a dummy equal to one if there is a decrease of NGOs' presence within the considered area of interest during Ebola. Sample (10-km + 1.42km internal buffer) restricted to be within the optimal bandwidth computed following the procedure outlined by Calonico et al., 2019. Moreover, due to potential dislocation of DHS respondents, 5km outside the area of interest have been eliminated by the sample. On the y-axis there are different weighting kernels. On the x-axis we show two group of results: (1) baseline, controlling only for SPEI; (2) controls, controlling also for rain and nightlights. Cell and region × year FE are added in all regressions. Standard errors clustered at the cell level. 90% confidence intervals shown.

deforestation, which is observable at a very granular level. Comparing cells just outside and just inside the palm oil area of interest, we find a severe increase in deforestation. We also document an increase of more than 125% in the likelihood of fire events within concessions during the epidemic. This deforestation was accompanied by a 65% increase in the amount of land dedicated to cultivation. Hence, the health crises has stimulated land grabbing by palm oil companies. This exploitative behaviour was highly profitable for them, with a 1428% increase in the value of Liberian palm oil's exports compared with the pre-Ebola period. We also highlight diversion of NGOs attention towards the epidemic. Consistently with this we find: (1) evidence of a strong decrease in the NGO presence within concessions during the crisis; (2) deforestation take place exactly in those areas interested by a reduction of NGOs presence. Overall, our results shows how a crisis may favour land grabbing behaviours in fragile countries and how attention/information may be important in preventing this negative outcomes. These results are extendable to extractive industries in Africa characterized by large concessions to (often multinational) companies by central governments, and some degree of competition between them and locals over (natural) resources.

References

Adler, R., Wang, J., Sapiano, M., Huffman, G., Chiu, L., Xie, P., … others (2016). Global precipitation climatology project (gpcp) climate data record (cdr), version 2.3 (monthly). *National Centers for Environmental Information*, *10*, V56971M6.

Ager, P., Eriksson, K., Karger, E., Nencka, P., & Thomasson, M. A. (2022). School Closures during the 1918 Flu Pandemic. *The Review of Economics and Statistics*, 1-28.

Bandiera, O., Buehren, N., Goldstein, M., Rasul, I., & Smurra, A. (2019). The economic lives of young women in the time of ebola: Lessons from an empowerment program. *World Bank Policy Research Working Paper*(8760).

Bian, B., Li, J., Xu, T., & Foutz, N. Z. (2022). Individualism during crises. *Review of Economics and Statistics*, *104*(2), 368–385.

Blankespoor, E., deHaan, E., & Marinovic, I. (2020). Disclosure processing costs, investors' information choice, and equity market outcomes: A review. *Journal of Accounting and Economics*, *70*(2-3), 101344.

Bonardi, J.-P., Gallea, Q., Kalanoski, D., Lalive, R., Madhok, R., Noack, F., … Sonno, T. (2021). Saving the world from your couch: The heterogeneous medium-run benefits of covid-19 lockdowns on air pollution. *Environmental Research Letters*.

Bradbury-Jones, C., & Isham, L. (2020). The pandemic paradox: The consequences of covid-19 on domestic violence. *Journal of clinical nursing*.

Brunetti, A., & Weder, B. (2003). A free press is bad news for corruption. *Journal of Public economics*, *87*(7-8), 1801–1824.

Calonico, S., Cattaneo, M. D., Farrell, M. H., & Titiunik, R. (2019). Regression discontinuity designs using covariates. *Review of Economics and Statistics*, *101*(3), 442–451.

Calonico, S., Cattaneo, M. D., & Titiunik, R. (2014). Robust nonparametric confidence intervals for regression-discontinuity designs. *Econometrica*, *82*(6), 2295–2326.

Chetty, R., Looney, A., & Kroft, K. (2009). Salience and taxation: Theory and evidence. *American economic review*, *99*(4), 1145–77.

Cleveland, D. A., & Cleveland, D. A. (2014). *Balancing on a planet: The future of food and agriculture* (Vol. 46). Univ of California Press.

Colella, F., Lalive, R., Sakalli, S. O., & Thoenig, M. (2019). Inference with arbitrary clustering.

Conley, T. G. (1999). Gmm estimation with cross sectional dependence. *Journal of econometrics*, *92*(1), 1–45.

Currie, J., Hanushek, E. A., Kahn, E. M., Neidell, M., & Rivkin, S. G. (2009). Does pollution increase school absences? *The Review of Economics and Statistics*, *91*(4), 682–694.

Davis, K. F., Yu, K., Rulli, M. C., Pichdara, L., & D Odorico, P. (2015). Accelerated deforestation driven by large-scale land acquisitions in cambodia. *Nature Geoscience*, *8*(10), 772–775.

DeHaan, E., Shevlin, T., & Thornock, J. (2015). Market (in) attention and the strategic scheduling and timing of earnings announcements. *Journal of Accounting and Economics*, *60*(1), 36–55.

Deininger, K., & Byerlee, D. (2011). *Rising global interest in farmland: can it yield sustainable and equitable benefits?* World Bank Publications.

DellaVigna, S. (2009). Psychology and economics: Evidence from the field. *Journal of Economic literature*, *47*(2), 315–72.

DellaVigna, S., & Pollet, J. M. (2009). Investor inattention and friday earnings announcements. *The Journal of Finance*, *64*(2), 709–749.

De Schutter, O. (2011). How not to think of land-grabbing: three critiques of large-scale investments in farmland. *The Journal of Peasant Studies*, *38*(2), 249–279.

Dhanani, L. Y., & Franz, B. (2020). Unexpected public health consequences of the covid-19 pandemic: a national survey examining anti-asian attitudes in the usa. *International Journal of Public Health*, *65*(6), 747–754.

Dimiceli, C., Carroll, M., Sohlberg, R., Kim, D., Kelly, M., & Townshend, J. (2015). Mod44b modis/terra vegetation continuous fields yearly l3 global 250 m sin grid v006. *NASA EOSDIS Land Processes Distributed Active Archive Center*.

Durante, R., & Zhuravskaya, E. (2018). Attack when the world is not watching? us news and the israeli-palestinian conflict. *Journal of Political Economy*, *126*(3), 1085–1133.

Eisensee, T., & Stromberg, D. (2007). News droughts, news floods, and us disaster relief. *The Quarterly Journal of Economics*, *122*(2), 693–728.

Emmanuel, S. C. (2000). Impact to lung health of haze from forest fires: the singapore experience. *Respirology*, *5*(2), 175–182.

Fetzer, T., Hensel, L., Hermle, J., & Roth, C. (2021). Coronavirus perceptions and economic anxiety. *Review of Economics and Statistics*, *103*(5), 968–978.

Fick, S. E., & Hijmans, R. J. (2017). Worldclim 2: new 1-km spatial resolution climate surfaces for global land areas. *International journal of climatology*, *37*(12), 4302–4315.

Gabaix, X., & Laibson, D. (2006). Shrouded attributes, consumer myopia, and information suppression in competitive markets. *The Quarterly Journal of Economics*, *121*(2), 505–540.

Galletta, S., & Giommoni, T. (2022). The effect of the 1918 influenza pandemic on income inequality: Evidence from italy. *Review of Economics and Statistics*, *104*(1), 187–203.

Global Witness. (2015). *The new snake oil? the violence, threats, and false promises driving rapid palm oil expansion in liberia.* (Tech. Rep.).

Grembi, V., Nannicini, T., & Troiano, U. (2016). Do fiscal rules matter? *American Economic Journal: Applied Economics*, 1–30.

Hansen, M. C., Potapov, P. V., Moore, R., Hancher, M., Turubanova, S. A., Tyukavina, A., … others (2013). High-resolution global maps of 21st-century forest cover change. *science*, *342*(6160), 850–853.

Johnston, F. H., Borchers-Arriagada, N., Morgan, G. G., Jalaludin, B., Palmer, A. J., Williamson, G. J., & Bowman, D. M. (2021). Unprecedented health costs of smoke-related pm 2.5

from the 2019–20 australian megafires. *Nature Sustainability*, *4*(1), 42–47.

Le Moglie, M., & Sorrenti, G. (2022). Revealing "mafia inc."? financial crisis, organized crime, and the birth of new enterprises. *Review of Economics and Statistics*, *104*(1), 142–156.

Londoño-Vélez, J., & Querubin, P. (2022). The impact of emergency cash assistance in a pandemic: Experimental evidence from colombia. *Review of Economics and Statistics*, *104*(1), 157–165.

Ludwig, J., & Miller, D. L. (2007). Does head start improve children's life chances? evidence from a regression discontinuity design. *The Quarterly journal of economics*, *122*(1), 159–208.

Marlier, M. E., DeFries, R. S., Voulgarakis, A., Kinney, P. L., Randerson, J. T., Shindell, D. T., … Faluvegi, G. (2013). El niño and health risks from landscape fire emissions in southeast asia. *Nature climate change*, *3*(2), 131–136.

Michaely, R., Rubin, A., & Vedrashko, A. (2016). Are friday announcements special? overcoming selection bias. *Journal of Financial Economics*, *122*(1), 65–85.

Nepstad, D. C., Verssimo, A., Alencar, A., Nobre, C., Lima, E., Lefebvre, P., … others (1999). Large-scale impoverishment of amazonian forests by logging and fire. *Nature*, *398*(6727), 505–508.

Nolte, K., Chamberlain, W., & Giger, M. (2016). International Land Deals for Agriculture. Fresh insights from the Land Matrix: Analytical Report II. *Land Matrix - Bern, Montpellier, Hamburg, Pretoria: Centre for Development and Environment, University of Bern; Centre de cooperation internationale en recherche agronomique pour le developpement; German Institute of Global and Area Studies; University of Pretoria; Bern Open Publishing*.

Patell, J. M., & Wolfson, M. A. (1982). Good news, bad news, and the intraday timing of corporate disclosures. *Accounting review*, 509–527.

Pellecchia, U., Crestani, R., Decroo, T., Van den Bergh, R., & Al-Kourdi, Y. (2015). Social consequences of ebola containment measures in liberia. *PloS one*, *10*(12), e0143036.

Peterman, A., Potts, A., O'Donnell, M., Thompson, K., Shah, N., Oertelt-Prigione, S., … others (2020). *Pandemics and violence against women and children* (Vol. 528). Center for Global Development Washington, DC.

Probst, B., BenYishay, A., Kontoleon, A., & dos Reis, T. N. (2020). Impacts of a large-scale titling initiative on deforestation in the brazilian amazon. *Nature Sustainability*, *3*(12), 1019–1026.

Rangel, M. A., & Vogl, T. S. (2019). Agricultural fires and health at birth. *Review of Economics and Statistics*, *101*(4), 616–630.

Tan, K. P., Kanniah, K. D., & Cracknell, A. P. (2014). On the upstream inputs into the modis primary productivity products using biometric data from oil palm plantations. *International Journal of Remote Sensing*, *35*(6), 2215–2246.

Appendix

A Extra-Figures

Figure A1: Palm Oil global price

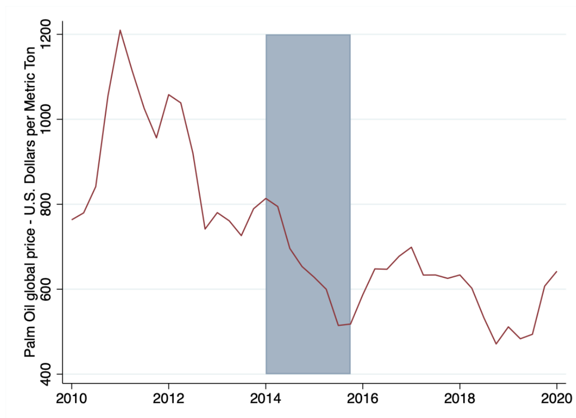

Notes: The figure presents the trend of palm oil global price (U.S. dollars per metric ton) over the period 2010-2020. Data from FRED. The blue area indicates the Ebola period as considered in this paper.

Figure A2: Percentage tree cover Liberia 2010

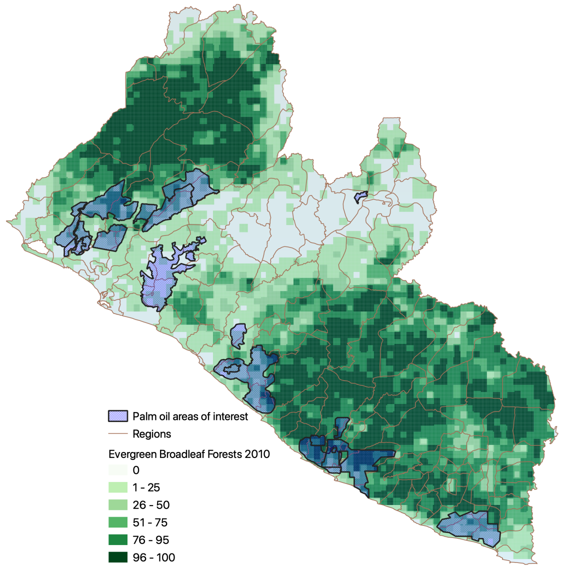

Notes: The figure presents the percentage of each cell covered by "Evergreen Broadleaf Forests" in 2010. The darker the cell, the higher the percentage. In blue we have the palm oil areas of interest and in gold the administrative boundaries of Liberia's regions. As the Figure shows, there is a low percentage belt in Evergreen Broadleaf Forest from Monrovia to the border with Guinea, given by the presence of "Savannas" in this area (see Figure A3 in the Appendix A).

Figure A3: Percentage tree cover Liberia 2010

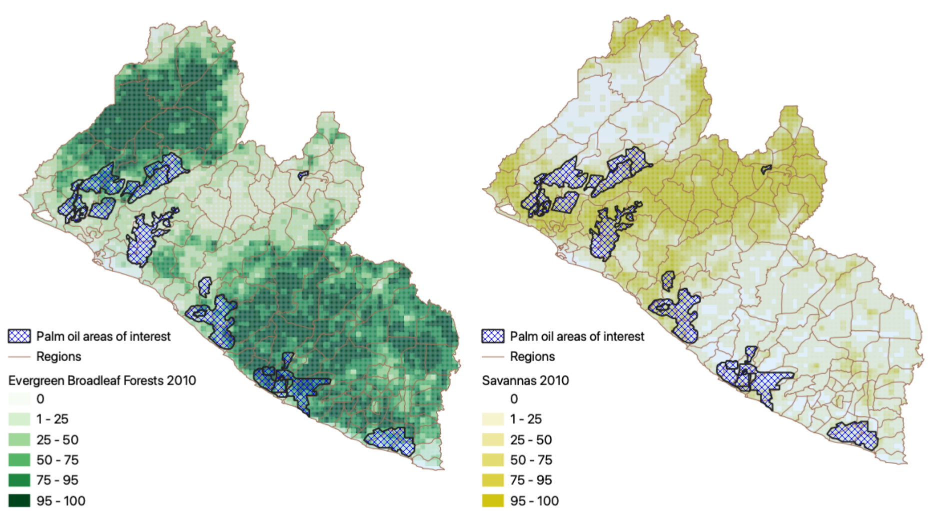

Notes: The figure presents the percentage of cell covered by "Evergreen Broadleaf Forests" on the right, and "Savannas" on the left in 2010 in Liberia. The darker is the cell, the higher the percentage of land cover by the IGBP class considered. In blue we have the Palm Oil Concessions and in gold the administrative boundaries of Liberia's regions.

Figure A4: 10km Sample

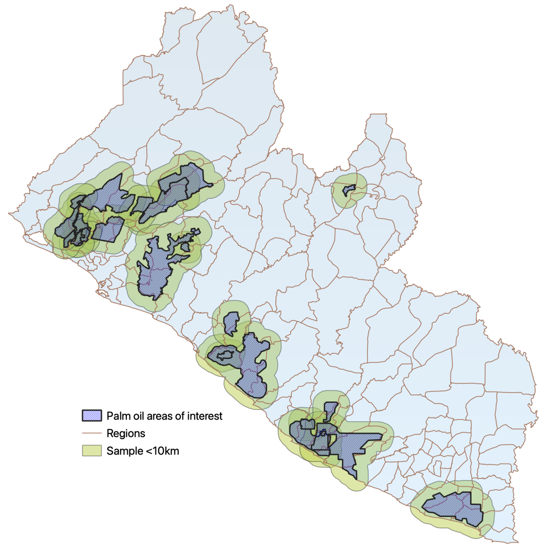

Notes: The figure presents sample used in the difference in discontinuities analysis.

Figure A5: Percentage tree cover Liberia 2010 MCD12Q1

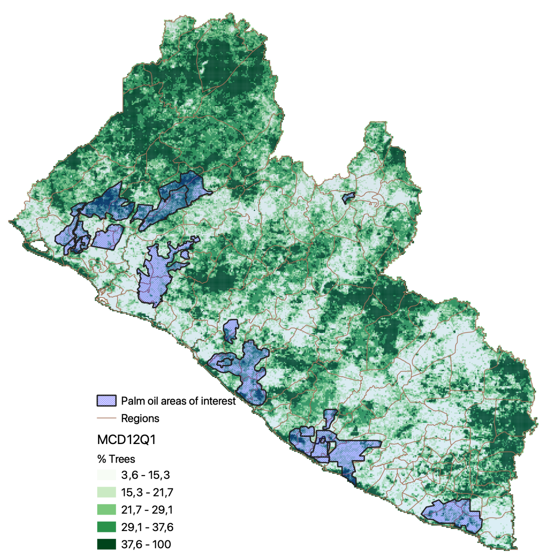

Notes: The figure presents the percentage of trees per each pixel in the MCD12Q1 data in 2010 in Liberia. The darker is the cell, the higher the percentage of tree cover. In blue we have the Palm Oil Concessions and in gold the administrative boundaries of Liberia's regions.

Figure A6: DHS respondent's locations

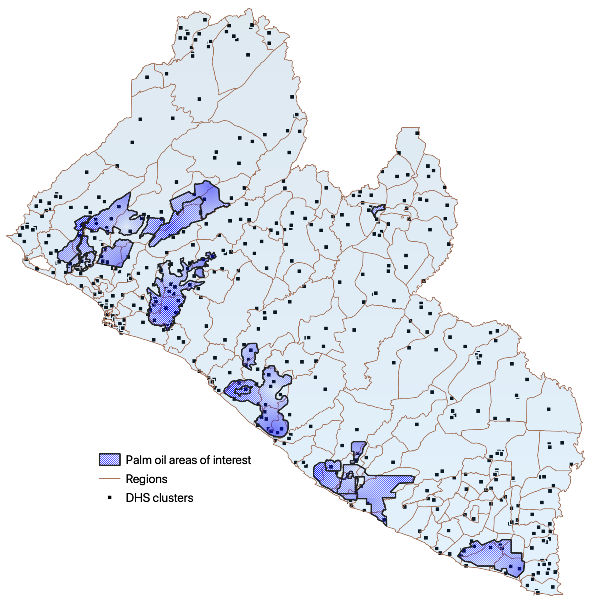

Notes: The figure presents the location of DHS respondent in the 3 waves used for NGO presence measurement (2011,2013, and 2016). In blue we have the Palm Oil Concessions and in gold the administrative boundaries of Liberia's regions.

B Extra-Tables

Table A1: Balances restricted sample before Ebola

	Outside Area of Interest	Within Area of Interest	Difference
Buffer, Bandwidth		*B = 0 km, h = 3 km*	
% Trees	40.107	40.080	-0.027
	(35.957)	(33.343)	(0.340)
SPEI	-0.094	-0.099	-0.005
	(0.953)	(0.954)	(0.009)
Fire event	0.007	0.008	0.002*
	(0.081)	(0.090)	(0.001)
% Crop	0.158	0.259	0.101***
	(1.114)	(1.258)	(0.012)
Observations	16,460	27,040	43,500
Buffer, Bandwidth		*B = 1.42 km, h = 3 km*	
% Trees	40.713	42.634	1.922***
	(36.209)	(32.313)	(0.486)
SPEI	-0.089	-0.089	0.000
	(0.963)	(0.980)	(0.014)
Fire event	0.007	0.007	0.000
	(0.083)	(0.084)	(0.001)
% Crop	0.139	0.196	0.058***
	(0.983)	(1.005)	(0.014)
Observations	10,560	9,580	20,140

Notes: Standard deviations in columns 1-2 and p-values in column 3. ***,**,* = indicate significance at the 1, 5, and 10% level, respectively.

Table A2: Sensitivity

	(1)	(2)
Dep. Variable	% Trees	Fire event
Baseline	-1.952	0.027
Std. clustered at cell level	(0.635)***	(0.013)**
Robust std.	(0.521)***	(0.012)**
Std. clustered at province level	(1.067)*	(0.019)
Conley std.	(0.819)**	(0.013)**
Nightlights	-1.971***	0.027**
	(0.634)	(0.013)
Population	-1.947***	0.027**
	(0.635)	(0.013)
Excluding SPEI	-1.850***	0.028**
	(0.635)	(0.013)
Rainfall	-2.071***	0.027**
	(0.635)	(0.013)
Rainfall (lag)	-1.923***	0.027**
	(0.636)	(0.013)
Temperature	-1.922***	0.028**
	(0.634)	(0.013)
Excluding Cell FE	-1.973***	0.027**
	(0.635)	(0.013)
Excluding Region × Year FE	-0.398***	0.106***
	(0.128)	(0.011)
Province FE × Year	-2.434***	0.027**
	(0.556)	(0.013)
Cell & Year FE	-2.330***	0.039***
	(0.662)	(0.014)
No weights	-1.933***	0.004
	(0.609)	(0.006)
Triangular kernel	-2.098***	0.012
	(0.796)	(0.007)
Uniform kernel	-1.933***	0.004
	(0.601)	(0.006)
Epanechnikov kernel	-2.161***	0.009
	(0.764)	(0.007)
Exclusion non-multinational company	-2.027***	0.039***
	(0.695)	(0.014)
MCD12Q1	-2.699***	
	(0.223)	

Notes: MWFE estimator. HDFE Linear regression. Standard errors in parentheses. ***,**,* = indicate significance at the 1, 5, and 10% level, respectively. Column (1) shows coefficient Ebola × Area of Interest of table 1, column (1), under different specifications. Column (3) shows the same coefficient but for model (3) of the same table. Column (2) shows coefficient Ebola × Area of Interest × Ethnic Minority of table 1, column (2), under different specifications. Column (4) shows the same coefficient but for model (4) of the same table. Conley std. with 250km of possible spatial correlation and 100 years of time correlation.

Table A3: Difference in discontinuities - sensitivity buffer

Dep. Variable	(1) % Trees	(2) Fire event
Panel A: Buffer radius = benchmark		
Ebola × Area of Interest	-1.952***	0.0277**
	(0.635)	(0.0134)
Observations	44577	155124
R-squared	0.980	0.209
Mean dependent	35.10	0.0223
Panel B: Buffer radius = 0km		
Ebola × Area of Interest	-1.952***	-0.000322
	(0.635)	(0.00771)
Observations	44577	154906
R-squared	0.980	0.201
Mean dependent	35.10	0.0233
Panel C: Buffer radius = 1.42km		
Ebola × Area of Interest	-0.909**	0.0277**
	(0.424)	(0.0134)
Observations	60471	155124
R-squared	0.979	0.209
Mean dependent	37.80	0.0223
Panel D: Buffer radius = 2km		
Ebola × Area of Interest	-0.932**	0.00907
	(0.366)	(0.0167)
Observations	137097	136559
R-squared	0.978	0.208
Mean dependent	38.93	0.0215

Notes: MWFE estimator. HDFE local linear regression. Sample restricted to be within the optimal bandwidth computed following the procedure outlined by Calonico et al., 2019. Observations weighted through an exponential kernel function of distance and bandwidth. Standard errors in parentheses. ***,**,* = indicate significance at the 1, 5, and 10% level, respectively. Standard errors clustered at the cell level in all models. Ethnic Minority is dummy equal one if a cell there is at least one politically unrepresented ethnic group, i.e. without representation in the government. Panels differ in the length of the buffer's radius. Only coefficients of interest shown in the table.

Table A4: NGO presence - difference of means

	(1)	(2)
Dep. Variable:	NGO	NGO
Area of Interest	0.010*	-0.002*
	(0.005)	(0.001)
Observations	686,861	196,246
Sample	No Ebola	Ebola
Mean dependent	0.00990	0.00153

Notes: MWFE estimator. HDFE local linear regression. Dependent variable is a dummy equal to 100 if, in the following year, in the cell-year there is at least one DHS respondent reporting an NGO spraying the dwelling against mosquitoes in the previous 12 months. *Area of Interest* is a dummy equal to one for cells in an area of interest. Standard errors in parentheses. ***,**,* = indicate significance at the 1, 5, and 10% level, respectively. Standard errors clustered at the cell level in all models.

Table A5: NGO presence

	(1)	(2)	(3)	(4)	(5)	(6)	(7)
Dep. Variable:	NGO	NGO	NGO	NGO	NGO	NGO	NGO
Ebola $\times$ Area of Interest	-0.00822***	-0.0146**	-0.0124*	-0.0188*	-0.0179*	-0.0179*	-0.0140**
	(0.000989)	(0.00684)	(0.00708)	(0.00970)	(0.00983)	(0.00983)	(0.00682)
Observations	883107	883107	882685	209097	208840	208840	820467
R-squared	0.000	0.115	0.115	0.112	0.112	0.112	0.116
Cell FE	No	Yes	Yes	Yes	Yes	Yes	Yes
Region $\times$ Year FE	No	Yes	Yes	Yes	Yes	Yes	Yes
Controls	No	No	Yes	No	Yes	No	Yes
Sample	Full	Full	Full	Diff-Disc	Diff-Disc	Displaced	Displaced
Mean dependent	0.00804	0.00804	0.00804	0.0134	0.0134	0.0134	0.00743

Notes: MWFE estimator. HDFE local linear regression. Dependent variable is a dummy equal to 100 if, in the following year, in the cell-year there is at least one DHS respondent reporting an NGO spraying the dwelling against mosquitoes in the previous 12 months. *Ebola* is a dummy equal to one in 2014 and 2015. *Area of Interest* is a dummy equal to one for cells in an area of interest. Standard errors in parentheses. ***,**,* = indicate significance at the 1, 5, and 10% level, respectively. Standard errors clustered at the cell level in all models. Models (1)-(3) use the full sample of all Liberia. Models (4)-(5) use the sample of the difference in discontinuities analysis (cells within 10km of the boundary of the areas of interest). Models (6)-(7) use a new sample excluding cells within 5km of the boundary. This is because the DHS, for privacy reasons, randomly dislocate locations of respondents by at most 5km in rural areas.

C Palm oil companies, cropland and palm oil

C.1 Description companies

In Liberia operate 7 large-scale palm oil companies, as outlined in table A6. The 23 *Areas of Interest* are not evenly distributed, with the largest MNE accounting for approximately 47% of them. These are quite large, with an average area of 377 km^2. Nevertheless, this mean hides substantial heterogeneity, as highlighted in figure A7. The majority of AoIs are indeed smaller than 160 km^2 (still an impressive figure). Then there is a long right tail of the area distribution, with the largest one being approximately 1300 km^2. Within these areas only the "owner" companies can operate, and cultivate. This address partially the issue concerning the Cropland classification in section 4.4. More on this in the next subsection. As discussed in 2, 6 out of 7 companies are part of large multinational groups. In particular, the largest 3 enterprises (in terms of number of areas of interest owned) are from groups with headquarters in Malaysia (a leading country in palm oil production), United Kingdom, and Hong Kong. The remaining company has access to only one, small (42 km^2), area. We were unable to understand whether this enterprise is entirely local or owned by other companies. Nevertheless, results are robust to the exclusion of this company, as shown in table A2. As for the age of these companies, they tend to be quite old. Indeed, the average foundation year, as shown in table A6, is 1977. The youngest company was created in 2010 and the oldest one in 1926. Consistently with this feature, and the Liberian history, the majority of these companies produced rubber before converting to palm oil.

Figure A7: Distribution area AoIs

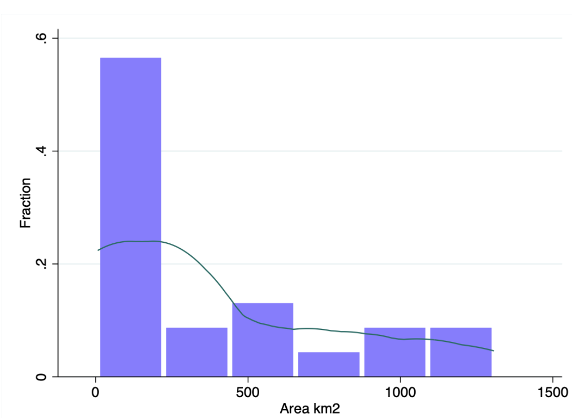

Table A6: Descriptives

Companies	7
Areas of Interest	23
- # AoIs 1st lagest MNE	11 ($\approx$ 47%)
- # AoIs 2nd lagest MNE	4
- # AoIs 3rd lagest MNE	3
Average area AoIs	377 km^2
Average foundation year	1977
Average % previously rubber	57%

C.2 Cropland and Palm oil

Newly planted palm oil trees are classified within as Cropland in the IGBP classification, as discussed by Tan et al. (2014) in Indonesia. However, of course, this is not the only tree type under in this class. Moreover, we cannot investigate what percentage of this category is actually constituted by these last ones. Indeed, to do so, we would need a more granular classification of different type of cultivation which, at the best of our knowledge, does not exists. Hence, one may be worried that results presented in the first paragraph of section 4.4 are driven by the increase of cultivation of other crops categorized in the same class. We think that this is not a substantial issue for three main reasons: (1) As said before, only palm oil companies are entitled to cultivate within these areas; (2) In turn, these companies can only plant palm oil trees, being these palm oil concessions, and this requirement is often explicitly written in their agreements with the central government; (3) The increase in palm oil trees is consistent with the 1428% increase in palm oil export in Liberia tree/four years after the Ebola outbreak (the time a plantation of palm oil need to become productive). Moreover, this increase in Liberian palm oil exports is not accompanied by any change in world palm oil price, consistently with this country not being a very large player in the world market (Figure A1).

D Other Data

For population data we use LandScan. This product was made utilizing the LandScan (2006-2018)TM High-Resolution global Population Data Set copyrighted by UT-Battelle, LLC, operator of Oak Ridge National Laboratory under Contract No. DE-AC05- 00OR22725 with the United States Department of Energy. The United States Government has certain rights in this Data Set. This dataset shows the number of inhabitants in 30-arc-second cells (about 1km $\times$ 1km near the Equator). In particular, LandScan aims to "develop a population distribution surface in totality, not just the locations of where people sleep". For this reason, it combines diurnal movements and travel habits in a single variable called *ambient-population*. To construct the data, it uses a "smart interpolation" technique combining census data, primary geospatial input, ancillary datasets, and high-resolution imagery analysis. We have imported these data, for each year, in Qgis as rasters and computed population statistics in each cell through the Qgis algorithm Zonal statistics, using this procedure for all the data since they all come as rasters, and we have to aggregate them at the cell level.

Temperature, Water Vapor Pressure, and Precipitation data come from WorldClim climate data for 1970-2000 (Version 2.1). We use these data to construct a measure of temperature and one of humidity. The authors collect monthly climate data for minimum, mean, and maximum temperature, precipitation, solar radiation, wind speed, water vapor pressure, and for total precipitation at the spatial resolution of our cells (Fick & Hijmans, 2017).

Rainfall data come from the Global Precipitation Climatology Project. See Adler et al. (2016). They provide estimated monthly rainfall data on a 2.5-degree global grid from 1979 to the present. As usual in the literature, we join these data to our cells and then take the average rainfall each year.

We add data on the Standardized Precipitation Evapotranspiration Index (SPEI), a multiscalar drought index that combines monthly precipitation and temperature data. These data are taken from the Global SPEI database based on monthly precipitation and potential evapotranspiration from the Climatic Research Unit of the University of East Anglia. This database offers long-term, robust information about drought conditions globally, with a 0.5 degree spatial resolution and a monthly time resolution.

E Descriptive Statistics

Table A7 reports some descriptive statistics for the whole period. Panel (a) shows the summary statistics for the total sample, Panel (b) focuses on areas of interest. A few elements are worth special notice. First, the mean percentage of tree cover is lower in areas of interest than in the full sample. This is as expected, as concessionaires must first deforest in order to plant palm oil trees. On the other hand, the average percentage of the cell consisting in cropland is more than twice as high in the areas of interest. This is reassuring as to data quality as well as the classification of palm oil trees. Second, there is no substantial difference in temperature pre-period, humidity pre-period, rainfall, SPEI, PM25, fire event, and temperature between cells inside and outside areas of interest. There is, however, a slight difference as regards population. In particular, the mean number of inhabitants is similar between the two categories, but the standard deviation in the cells outside the areas of interest is approximately four times as great as inside (reflecting the fact that cities are found only outside these areas). Third, as Panel (a) shows, approximately 10% of the cells are in areas of interest, and in fact Panel (b) has about 10% as many observations as Panel (a). This is an impressive figure. The total land area covered by concessions is approximately 10 thousands km^2. To put things into perspective, this figure is larger than the total surface of a small country like Cyprus. Fourth, consistently with anecdotal evidence suggesting that NGOs helped communities within areas of interest, the mean of NGOs' presence is higher in Panel (b).

Table A7: Descriptive Statistics

	Obs.	Mean	S.D.	Min	Max
Panel (a): All Sample					
% Trees	881,883	48.12451	37.97548	0	100
% Crop	881,883	.1537871	1.039155	0	25
Area of Interest	883,107	0.0997	0.300	0	1
Fire event	881,365	0.0232	0.150	0	1
SPEI	882,045	-0.0972	0.880	-2.421	1.832
Population	882,685	38.40	441.0	0	51,859
Humidity pre-period	880,497	0.0542	0.00304	0.0495	0.0637
Rain	883,107	210.1	46.72	-4,297	461.8
Pm 25	882,702	33.21	4.488	22.30	45.60
Nightlights	883,107	0.294	1.551	0	45.12
Temperature	883,035	27.75	0.580	23.86	29.90
NGO	883,107	.0080398	.8966135	0	100
Panel (b): Areas of Interest					
% Trees	88,056	37.38392	31.74739	0	100
% Crop	88,056	.436153	1.67144	0	17
Fire event	87,988	0.0222	0.147	0	1
Population	88,043	37.57	141.5	0	5,675
Humidity pre-period	88,029	0.0569	0.00272	0.0505	0.0635
Rain	88,056	235.4	40.91	142.0	407.8
SPEI	87,975	-0.0739	0.802	-2.421	1.832
Pm 25	88,056	32.44	4.452	22.70	43.60
Nightlights	88,056	0.417	1.676	0	25.81
Temperature	88,056	27.76	0.646	26.34	29.72
NGO	88,056	.0147633	1.214962	0	100

F Sharp Geographic Regression Discontinuity

An alternative to the difference in discontinuities approach, more common although not perfect for this context, is a simple sharp geographic regression discontinuity identification strategy. In this case we simply compare cells at the areas of interests' boundaries. The basic idea behind this method is to compare cells just outside and inside palm oil areas of interest. Indeed, given their proximity, they are very likely to be similar. However, multinational companies may have rapacity behaviour only in cells inside the area of interest. Hence, comparing these two groups, one could recover the effects on our dependent variables. An immediate, and resolutive, limitation of this approach is that it ignores totally the time dimension, which instead is crucial in the natural experiment presented in Section 2. In the following section, we present results using this approach.

As in the difference in discontinuities analysis presented in Section 4, we first restrict our sample to those cells within the 10 km radius around areas of interests boundaries. Then, we apply an internal buffer of 1.42 km to both sides of the areas to deal with noisiness produced by geographic measures.

To estimate the local linear regression discontinuity treatment effect we follow the procedure outlined by Calonico et al. (2019). We run local linear regressions of Y_{krt} on a constant, a dummy indicating areas of interest A_{kr}, the distance D_k and their interaction, using only units within bias robust and optimally chosen bandwidths ($D_k \in [-h, h']$), and weighting observations through a kernel function according to their distance from the cutoff.[18]

$$Y_{krt} = \alpha + \tau A_{kr} + \beta D_k + \gamma A_{kr} \times D_k + u_{krt} \tag{4}$$

Table A8 presents results differentiating between Ebola periods and non Ebola ones. Results are consistent with the ones outlined before: during the health crisis, there is a lower percentage of trees within areas of interest, an higher probability of experiencing a fire event, and these effects are larger when considering areas populated by ethnic minorities. Interestingly, both coefficients of interest τ and its interaction with the ethnic dimension are statistically different from 0 only during Ebola periods. This is also true when

[18] Specifically, the exponential kernel function is of the form: $K(D/h) = \frac{e^{h-|D|}}{e}$.

analysing the probability of observing a fire event in columns 5 and 6 of the table. These results suggest that being within an area of interest, although usually associated with a lower percentage of tree coverage, makes truly a difference at the border only during the Ebola period.

Table A8: Sharp geographic regression discontinuity

	(1)	(2)	(3)	(4)	(5)	(6)	(7)	(8)
Dep. Variable	% Trees	% Trees	% Trees	% Trees	Fire event	Fire event	Fire event	Fire event
Area of Interest	-4.094***	-2.978	0.166	-3.403	0.0249*	-0.00173	-0.0859**	-0.0199**
	(1.579)	(2.055)	(1.488)	(2.783)	(0.0132)	(0.00209)	(0.0379)	(0.00911)
Distance	-1.663***	-1.858***	-0.677**	-1.205	0.000923	0.000137	0.0118	-0.000581
	(0.304)	(0.533)	(0.299)	(1.155)	(0.00235)	(0.000374)	(0.0114)	(0.00146)
Ethnic Minority			-0.534	-3.116			-0.0245	-0.0108
			(1.559)	(2.929)			(0.0386)	(0.00953)
Distance × Area of Interest	1.916***	2.308***	0.728**	1.764	-0.0119***	0.000688	-0.00999	0.00217
	(0.523)	(0.802)	(0.313)	(1.154)	(0.00422)	(0.000677)	(0.0111)	(0.00170)
Ethnic Minority × Area of Interest			-6.311***	0.487			0.115***	0.0187**
			(1.806)	(3.514)			(0.0403)	(0.00938)
Ethnic Minority × Distance			-0.679**	-0.684			-0.0115	0.000738
			(0.321)	(1.282)			(0.0117)	(0.00151)
Ethnic Minority × Distance × Area of Interest			0.722*	0.511			-0.00113	-0.00149
			(0.400)	(1.432)			(0.0120)	(0.00183)
Observations	30510	54341	30510	54341	34474	120650	34474	120650
R-squared	0.523	0.533	0.548	0.533	0.0858	0.0127	0.0869	0.0131
Region × Year FE	Yes	Yes	Yes	Yes	Yes	Yes	Yes	Yes
SPEI	Yes	Yes	Yes	Yes	Yes	Yes	Yes	Yes
Sample	Ebola	No Ebola	Ebola	No Ebola	Ebola	No Ebola	Ebola	No Ebola
Mean dependent	37.54	37.98	39.52	37.98	0.0781	0.00634	0.0781	0.00634

Notes: MWFE estimator. HDFE local linear regression. Sample restricted to be within the optimal bandwidth computed following the procedure outlined by Calonico et al., 2019. Observations weighted through an exponential kernel function of distance and bandwidth. Standard errors in parentheses. ***,**,* = indicate significance at the 1, 5, and 10% level, respectively. Standard errors clustered at the cell level in all models. Ethnic Minority is dummy equal one if a cell there is at least one politically unrepresented ethnic group, i.e. without representation in the government.

The identification assumption in this case is the continuity of potential outcomes' conditional means at the boundaries: in the absence of treatment, the average three coverage of cells just outside and inside palm oil areas of interest should have been the same. In other words, cells should be almost randomly allocated at the boundaries. However, this is not the case. Areas of interest boundaries are not random; they have been decided in the past based on some unobserved characteristics. This could lead to a possible violation of the continuity assumption. Moreover, the setting explained in section 2 requires comparing periods during the health crises with those before the Ebola outbreak. This means that we need to compare trends and not levels. In addition to that, comparing trends also offsets the first limitation outlined before since one takes out all unobserved characteristics that are unchanged over time of each cell. These are exactly those characteristics that, likely, have driven to the areas of interests' drawing decisions, such as the suitability of soil. For these reasons the difference in discontinuities approach is much more robust in this analysis than the one presented in this section.

G Identification

In this section we will look in detail at the identification procedure of the difference in discontinuities (Calonico et al., 2014, Ludwig & Miller, 2007, Grembi et al., 2016). Let t=0,1 be the time, t=0 no-Ebola and t=1 Ebola. Let $Y_t(p)$ be the potential outcome p=0,1 of the percentage of three cover of a generic cell at time t=0,1. Our goal is to identify the following:

$$\mathbb{E}\{Y_1(1) - Y_1(0)|X = 0\} \tag{5}$$

where X is the distance from the concession boundaries (negative values of X indicate that the cell is *outside* the area of interest). This is the average treatment effects at the area's boundaries during Ebola. A simple sharp regression discontinuity approach would have assumed continuity of potential outcomes:

$$\mathbb{E}\{Y_1(1)|X\}, \mathbb{E}\{Y_1(0)|X\} \text{ both continuous at } X = 0$$

and identified 5 by taking

$$\text{ATEc} = \lim_{x \to 0^-} \mathbb{E}\{Y_1|X = x\} - \lim_{x \to 0^+} \mathbb{E}\{Y_1|X = x\}$$

Here we make two different assumptions that take advantage of the time dimension.

Assumption 1. $\mathbb{E}\{Y_t(p)|X\}$ *is right continuous* $\forall t, p$ *for* $X > 0$ *and left continuous* $\forall t, p$ *for* $X < 0$

Assumption 2. $\lim_{x \to 0^-} \mathbb{E}\{Y_1(0)|X = x\} - \lim_{x \to 0^-} \mathbb{E}\{Y_0(0)|X = x\} = \lim_{x \to 0^+} \mathbb{E}\{Y_1(0)|X = x\} - \lim_{x \to 0^+} \mathbb{E}\{Y_0(0)|X = x\}$ *that is our new parallel trend assumption at the threshold.*

Assumption 1 is weaker than continuity because it does not require potential outcomes to be continuous across the threshold but only right and left continuous respectively at the right and at the left of the threshold. In other words, potential outcomes could be highly discontinuous at the threshold, a condition that would violate the internal validity of the regression discontinuity approach. Though we need this weaker version of continuity because we need to take the limits of these expectations as the running variable approaches to the threshold and, hence, we need to be sure that such limits exists. Assumption 2 resemble the parallel trend assumption seen in the difference in difference approach. However, it is much weaker. Indeed, we do not assume that, on average, trends of *all* the treatment and control group would have been the same in absence of treatment. We only assume that this is the case for cells very close to each other, because both are very close to the threshold. Hence, assumption 2 is more likely to be satisfied than the classic parallel trend assumption. The identification theorem follows.

Theorem G.1. *In difference-in-discontinuities, under assumptions 1 and 2, ATE at the threshold* $\mathbb{E}\{Y_1(1)-Y_1(0)|X=0\}$ *is identified by*

$$\beta = \lim_{x\to 0^-} \{\mathbb{E}\{Y_1|X=x\} - \mathbb{E}\{Y_0|X=x\}\} - \lim_{x\to 0^+} \{\mathbb{E}\{Y_1|X=x\} - \mathbb{E}\{Y_0|X=x\}\}$$

Proof. To prove theorem G.1 notice that observed potential outcomes are:

$$\begin{aligned} &Y_0(0) \quad \forall x \in \chi \\ &Y_1(1) \quad \forall x \geq 0 \\ &Y_1(0) \quad \forall x < 0 \end{aligned}$$

Substituting them in our expression we get:

$$\beta = \lim_{x\to 0^-} \{\mathbb{E}\{Y_1(1)|X=x\} - \mathbb{E}\{Y_0(0)|X=x\}\} - \lim_{x\to 0^+} \{\mathbb{E}\{Y_1(0)|X=x\} - \mathbb{E}\{Y_0(0)|X=x\}\}$$

where we can take limits thanks to assumption 1. Substituting assumption 2 we get the following:

$$\beta = \lim_{x\to 0^-} \{\mathbb{E}\{Y_1(1) - Y_1(0)|X=x\}\} = \mathbb{E}\{Y_1(1) - Y_1(0)|X=0\} = \text{ATEc}$$

□

H Ethnic minorities

In this section we explore the heterogeneity of our results with the presence of ethinc minorities in the area. Specifically, we enrich our models 1 and 2 with an additional interaction, namely a dummy equal to one if in a cell there is at least one politically unrepresented ethnic group, i.e. without representation in the government. This specification confirms that during the Ebola epidemic, deforestation was more intense in areas inhabited by unrepresented ethnic groups as one can see in table A9, column 1. Simultaneously, we observe an higher probability of observing a fire event (column 2). Results are qualitatively similar when turning to the difference in discontinuity approach (columns 3 and 4).

Table A9: Difference in Difference and Difference in Discontinuities

	Diff in Diff		Diff in Disc	
	(1)	(2)	(3)	(4)
Dep. Variable	% Trees	Fire event	% Trees	Fire event
Ebola × Area of Interest	2.556***	-0.0529***	0.318	-0.0614*
	(0.0474)	(0.00430)	(1.322)	(0.0336)
Ebola × Area of Interest × Ethnic Minority	-1.376***	0.0732***	-2.419	0.0935**
	(0.0688)	(0.00465)	(1.479)	(0.0364)
Observations	880821	880357	44577	155124
R-squared	0.966	0.228	0.980	0.209
Cell FE	Yes	Yes	Yes	Yes
Region × Year FE	Yes	Yes	Yes	Yes
SPEI	Yes	Yes	Yes	Yes
Mean dependent	48.15	0.0232	35.10	0.0223

Notes: MWFE estimator. HDFE local linear regression. Sample restricted to be within the optimal bandwidth computed following the procedure outlined by Calonico et al., 2019. Observations weighted by an exponential kernel function of distance and bandwidth. Standard errors in parentheses. ***,**,* = indicate significance at the 1, 5, and 10% level, respectively. Standard errors clustered at the cell level in all models. *Ebola* is a dummy equal to one in 2014 and 2015. *Area of Interest* is a dummy equal to one for cells in an area of interest. *Ethnic Minority* is dummy equal one if in a cell there is at least one politically unrepresented ethnic group, i.e. without representation in the central government.